Int. J. Pharm. Investigation, 2026; 16(4):1696-1718.
https://www.jpionline.org

Original Article

Computational Simulation of Monoamine Oxidase (PDB ID: 2BXR) "Molecular Docking, Molecular Dynamics, and 3D-QSAR Analysis of 10H-Phenothiazin-1-yl Derivatives Targeting Enzymes"

Sanket Keshav Tambe[1,*], Rohit Jaysing Bhor[1], Sagar Dattatray Magar[1], Mayur Shivaji Bhosale[1], Shubham Popatrao Mankar[1], Datta Macchindra Abhale[3], Sachin Tukaram chavan[4], Gaurav Subhash Damre[2]

[1]Department of Pharmaceutical Chemistry, Pravara Rural College of Pharmacy, Pravaranagar, Rahata, Ahmednagar, Maharashtra, INDIA.
[2]Department of Pharmacy Practices, Pravara Rural College of Pharmacy, Pravaranagar, Rahata, Ahmednagar, Maharashtra, INDIA.
[3]Department of Quality Assurance, Dr. Kolpe Institute of Pharmacy, Kolpewadi, Kpoergaon, Ahilayanagar, Maharashtra, INDIA.
[4]Department of Pharmacognosy, Dr. Kolpe Institute of Pharmacy, Kolpewadi, Kpoergaon, Ahilayanagar, Maharashtra, INDIA.

ABSTRACT

Background: This study focuses on the computational (in silico) analysis of 1H-phenothiazine derivatives to estimate their pharmacological potential, particularly as inhibitors of monoamine oxidase (PDB ID: 2BXR), an enzyme linked to depression. Using assorted computational methods, the study investigates structure-activity relationships and predicts the impact of structural changes on drug effectiveness. Results show that several compounds demonstrated significant cytotoxic activity against depression-related targets, suggesting promising inhibitory and anti-inflammatory properties. This work attempts to examine the inflammatory and enzyme-inhibitory properties of a novel series of 1H-phenothiazin derivatives in order to determine whether they may be used as multi-action therapeutic drugs. Combi Lab studies and 3D-QSAR were carried out using the Molecular Design Suite. Molecular docking analysis was conducted using Schrodinger Maestro. Out of the sixteen compounds made utilizing a Combinatorial technique, five compounds (PS6; PS5; PS11; PS13, and PS15) showed greater projected biological activity compared to the dataset's most active molecule. The amino acid residues on monoamine oxidase (PDB ID: 2BXR) (PDB: 3LN1), including Val-349, Tyr-385, Phe-518, Trp-387, Gly-526, Tyr348, Met-522, Leu-352, Phe381, Leu-384, and Tyr-385 were in close proximity to these substances.

Keywords: ADMET, Depression, Molecular docking, COX-1 (PDB: 3KK6) and Monoamine oxidase (PDB ID: 2BXR) (PDB: 3LN1), Phenothiazine.

Correspondence:
Mr. Sanket Keshav Tambe
Department of Pharmaceutical Chemistry, Pravara Rural College of Pharmacy, Pravaranagar, Rahata, Ahmednagar, Maharashtra, INDIA.
Email: Sankettambe77.st@gmail.com
ORCID: 0009-0000-6105-9135

Received: 11-05-2026;
Revised: 03-06-2026;
Accepted: 29-07-2026.

INTRODUCTION

Current antidepressants usually work by affecting brain chemicals like serotonin and noradrenaline, which are essential for mood regulation (Babalola *et al*., 2021; Hu *et al*., 2015). The most commonly used drugs involve selective serotonin reuptake inhibitors such as fluvoxamine, citalopram, fluoxetine, escitalopram, as well as noradrenaline reuptake inhibitors like desipramine. Drug discovery is a very complex and costly process that involves choosing a disease, identifying and confirming the right targets, finding and improving lead compounds, and then testing them through preclinical and clinical trials (Hamama *et al*., 2020). Research has shown that many drug candidates fail because of poor pharmacokinetic profiles and ADMET properties. This has made it important to assess "drug-likeness" (Hamama *et al*., 2022) early on in the development process. Computer-based methods are now key in early drug discovery to help predict and reduce the risk of toxicity. Phenothiazine has been widely used in medicinal chemistry, and its derivatives are known for various activities, including antipsychotic and antidepressant effects (Adetobi *et al*., 2022; Femi-Olabisi *et al*., 2021). A popular method for forecasting how a tiny molecule would behave is called molecular docking (drug) fits into the binding site of a protein, offering insights into both the binding shape and strength (Batiha *et al*., 2023). This method is very useful for both screening potential drug candidates and analyzing how well lead compounds might work. It might be difficult to treat multifactorial illnesses since they frequently have several underlying causes (Barbosa *et al*., 2020). There is a lot of promise

OPEN ACCESS
Manuscript TECHNOMEDIA

DOI: 10.5530/ijpi.20260011

for treating a wide range of illnesses by creating innovative hybrid molecules with a variety of pharmacological actions that can alter different biochemical pathways (Boehm *et al.*, 1996). Despite the tremendous Designing and optimizing such compounds is challenging (Al Zahrani *et al.*, 2020; Bansode *et al.*, 2014), compared to medicine combinations or multicomponent therapies, this method has clear advantages because it lowers the possibility of drug interactions. Olanzapine, aripiprazole, and risperidone are examples of atypical antipsychotics that primarily work as dopamine and serotonin receptor antagonists (Akinwande *et al.*, 2014), showing a relatively low affinity for α-adrenergic, cholinergic muscarinic, and histaminergic receptor subtypes (Ben-Levy *et al.*, 1998). One of the exciting advances in drug discovery is the coordinated combination of several beneficial moieties on identical substances, especially for the treatment of certain illnesses (Chan *et al.*, 2017). The ideal environment for creating novel compounds with pleiotropic pharmacological effects is in the area of pharmaceutical benefits that reduce the need for polypharmacy, such as treatments that also reduce iatrogenic side effects, prevent symptoms, or enhance beneficial effects through adjuvant therapeutic mechanisms (Cuadrado & Nebreda, 2010). Dual inhibitors frequently have high atomic weights, which may reduce the possibility of their therapeutic effects. As a result, pharmacokinetic properties and safety profiles need to be carefully considered while constructing dual inhibitors (Field *et al.*, 2018). The heterocyclic aromatic organic substance phenothiazine is produced when imidazole and benzene are combined. Because of their numerous impacts, they have been important in medical chemistry because of their analgesic, anti-tumour, antiviral, and psychotropic qualities (Akinwande *et al.*, 2023; Gröber *et al.*, 2013). The complex biochemical response of body tissues to infections is an immune cell-defined mechanism (Hobbenaghi *et al.*, 2013). Monoamine oxidase (PDB ID: 2BXR) Enzyme: (COX), which comes in the forms Monoamine oxidase (PDB ID: 2BXR) Enzyme: is a crucial protein required to produce prostaglandins from arachidonic acid. While MONOAMINE OXIDASE (PDB ID: 2BXR) (PDB: 3LN1) is created in response to inflammatory stimuli, COX-1 (PDB: 3KK6) provides prostaglandins (Horiuchi *et al.*, 1999). In human cancers, MONOAMINE OXIDASE (PDB ID: 2BXR) (PDB: 3LN1) contributes to cell division, angiogenesis, and death. Molecular docking, a method for determining the interaction between a protein and ligand, describes the orientation, binding interactions, and binding energy of the molecule (Kumar *et al.*, 2003). Pharmacophore techniques are necessary to predict the common molecular traits of those involved in the molecular-level interactions involving biological targets (Lee & Young, 1996). The aim of this study was to analyse the physicochemical and ADMET properties of the synthesized drugs and identify the molecular interactions in COX and phenothiazine analogues (Ono & Han, 2000). Furthermore, unique characteristics were investigated through pharmacophore modelling studies. Given the claimed anti-depressant activity properties of phenothiazine derivatives, it is crucial to illustrate their mechanism of action (Ramesh *et al.*, 2014). To determine the in silico inhibitory impact of such compounds, were docked with Monoamine oxidase (PDB ID: 2BXR) Enzyme: In order to determine how phenothiazine function to inhibit Monoamine Oxidase (pdb id: 2bxr) enzymes, which is what gives them their Anti-Depressants Activity properties, in silico research is necessary. An essential mechanism against all types of chemical, physical, and viral attacks is depression (Rathod *et al.*, 2016). The body experiences pathological situations as organ rejection, autoimmune disorders, and allergies when this pathway is dysregulating (Streit *et al.*, 2004). NSAIDs are widely utilized by millions of people around the world for their ability to alleviate pain, reduce fever, and manage inflammation. These drugs exert their effects by inhibiting enzyme monoamine oxidase (PDB ID: 2BXR), which in turn prevents the conversion of arachidonic acid into pro-inflammatory molecules like prostaglandins and Thromboxanes (TXs). In 1997, Needleman and Isakson published the first description of two isoenzyme. The "House Keeping" enzyme, monoamine oxidase (PDB ID: 2BXR), Numerous things can cause the "inducible" enzyme to produce inflammatory reactions. The specific functions of the monoamine oxidase isoform (PDB ID: 2BXR), which is uniquely expressed in certain regions of the Central Nervous System (CNS), remain unclear. In response to pro-inflammatory and pathogenic stimuli, notably phorbol esters, lipopolysaccharides, and cytokines, second monoamine oxidase (pdb id: 2bxr) is generated. The release of PGs and depression are both caused by the monoamine oxidase (pdb id: 2bxr) enzyme. Monoamine oxidase (PDB ID: 2BXR) has been connected in numerous studies to a variety of clinical conditions, including depression, neurological diseases, and cancer. Hence, it is also used to treat cancer. Selective monoamine oxidase (PDB id: 2bxr) (PDB: 3LN1) inhibitor drugs, such as celecoxib, rofecoxib, and valdecoxib, were developed to lessen these severe adverse effects. These drugs have better gastrointestinal safety profiles and the same analgesic effects as non-selective monoamine oxidase (pdb id: 2bxr) inhibitors. Unfortunately, as they have adverse effects on Monoamine oxidase (pdb id: 2bxr) pathway, with a higher risk of myocardial infarction and high blood pressure, both rofecoxib and valdecoxib have been taken off the market. The adverse side effects of rofecoxib and valdecoxib were linked to their different chemical compositions. Because of this, research is still being done to find selective antidepressant activity drugs that have better safety profiles than the NSAIDs currently on market. Derivatives of inhibition were tested in the monoamine oxidase (PDB ID: 2BXR) enzyme. Subsequently, to elucidate their potential mode of action, the synthesized compounds docked into the monoamine oxidase (pdb id: 2bxr) enzyme site.

MATERIALS AND METHODS

Molecular docking and the synthesis of ligands

Test compounds PS1-PS16 structures and the phenothiazine scheme were provided in Figure 1 and Table 1 prior to molecular docking. Using the ArgusLab 4.0.1 software and the semi-empirical method, we optimized. Preparing proteins for docking investigations, we employed a range of distinct monoamine oxidase (PDB ID: 2BXR) enzyme crystal structures from the RCSB. The study examined the compounds' ADMET, physicochemical properties, and drug similarity. PDB provided the monoamine oxidase ribbon composition (PDB ID: 2BXR). An enzyme 1.5.6 was the version of auto dock. The selection was Chain A. After removing the water, polar hydrogen with Gasteiger charges was added. The grid map was their choice. ChemDraw Ultra 12.0 was utilized to create the 2D formula for the compounds. Utilizing Avogadro software, energy consumption was reduced. Discovery Studio was used to visualize the reactions, and Auto dock Vina was utilized to implement the docking technique. Optimising the docking method involved comparing the crystal structures of Celecoxib (CEL) with the expected conformations of the docking statistics. In Figure 2, the Ribbon Structure Protein structure's crystalline form was superimposed, and in Figure 3, a Ramachandran plot was exhibited.

RESULTS

Lipinski's rule of five and molecular docking

Lipinski's "rule of five"-A experimental and computational approach for calculating permeability as well as solubility -is followed throughout the drug development process. PDB ID for monoamine oxidase: 2BXR Enzyme: medicines and enzymes were docked, and the molecular interactions between the two were analysed. The 2D-3D Composition for molecular bindings are shown in Table 2 summarizes Chemical processes involving dynamic amino acid residues. While lead optimization and identification have historically been the main focus of Computer-Aided Molecular Design (CAMD), a number of innovative methods have been developed for helping strengthen "binding affinities of drug candidates to particular receptors. These overall guidelines evaluate a molecule's drug-likeness and determine whether it possesses pharmacological action. The rule was based on the observation that certain lipophilic molecules, which make up the majority of medications, perform best when given orally. It is used when the pharmacologically active lead compound is iteratively enhanced to increase their activity and selectivity while preserving its" drug-like physical and chemical properties in the process of creating novel medications. Rotation of bonds, Table 3 includes data on H-bond donors and acceptors, as well as violations of the Lipinski, Ghose, Veber, Egan, and Muegge rules. To make oral drugs that work, chemicals must have ADMET properties. A ligand's toxicity is believed to be necessary for it to serve as an effective tool, and Qik-Prop generates descriptions that are physically significant. The ligand preparation tool used in research is the Ligprep module. The protein preparation wizard is used to prepare proteins. Monoamine oxidase's X-ray crystal structures are obtained from the PDB data bank. An enzyme: grid produced by the Receptor Grid Generation Wizard. The Figure 4 provided by the Receptor Grid Generation Wizard. The ligand and protein were connected by Glide XP, and interactions were observed. The scoring function allocates points based on the ideal

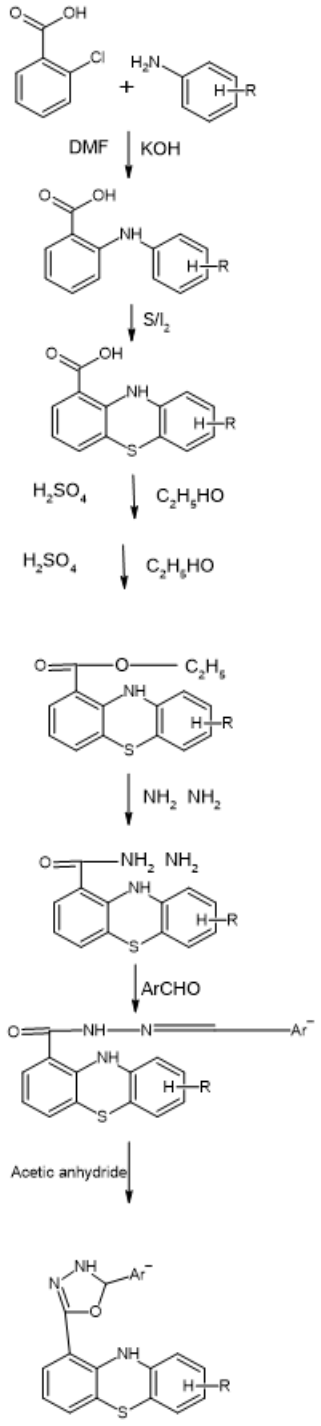

Figure 1: Scheme of Phenothiazine.

Table 1: Derivatives of Designed Compound of Phenothiazine.

COMP. CODE	Ar	R	COMP. CODE	Ar	R
PS1	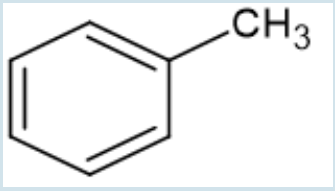	Cl	PS16	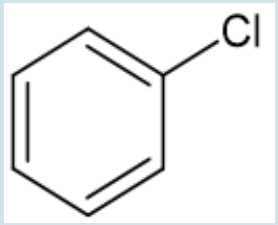	Cl
PS2	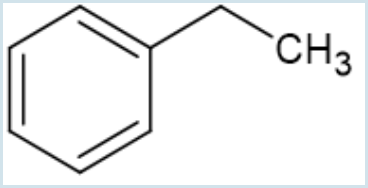	Cl	PS17	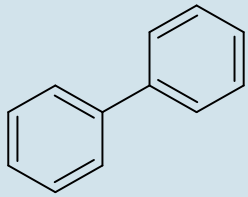	Cl
PS3	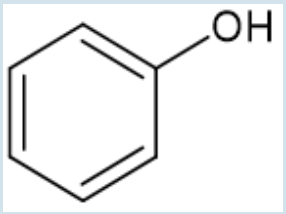	Cl	PS18	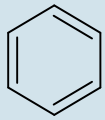	Cl
PS4	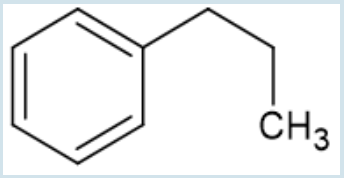	Cl	PS19	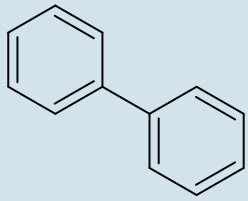	Cl
PS5	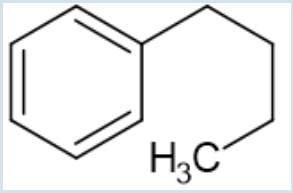	Cl	PS42	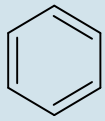	Br
PS6	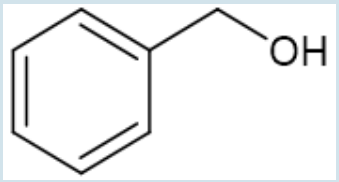	Cl	PS44	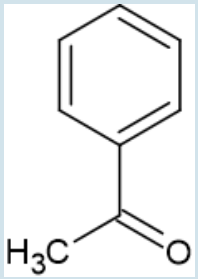	Br
PS7	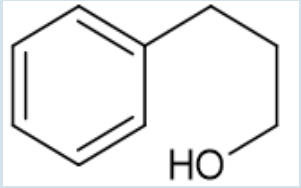	Cl	PS45	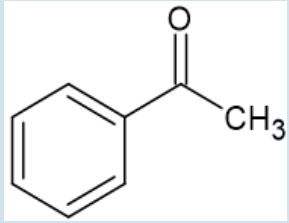	Br

PS8	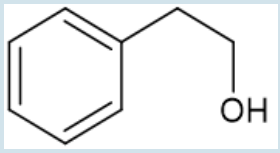	Cl	PS46	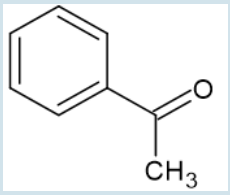	Br
PS9	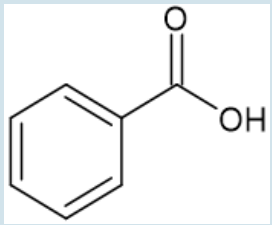	Cl	PS47	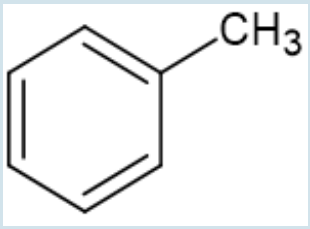	NO2
PS10	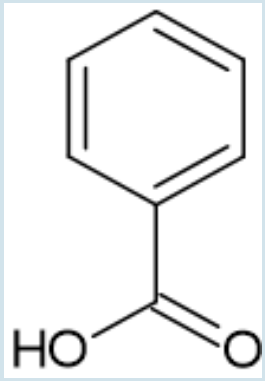	Cl	PS51	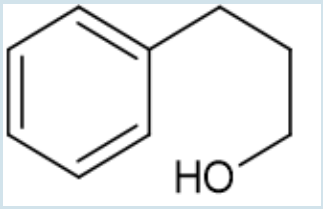	NO2
PS11	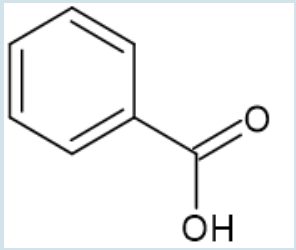	Cl	PS52	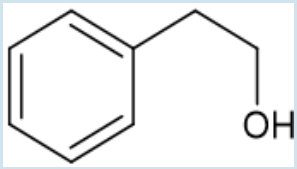	NO2
PS12	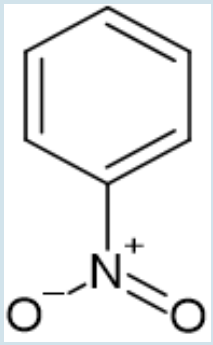	Cl	PS53	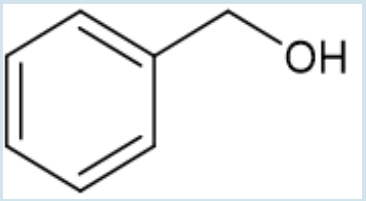	NO2
PS13	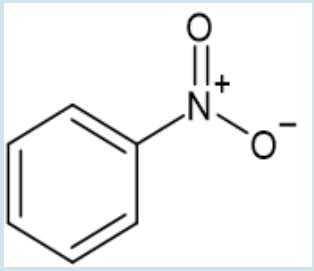	Cl	PS54	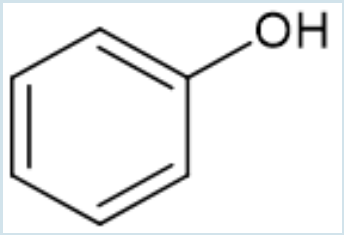	NO2

PS14	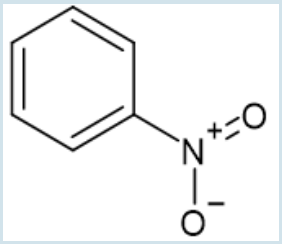	Cl	PS62	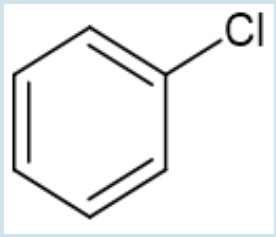	NO2
PS15	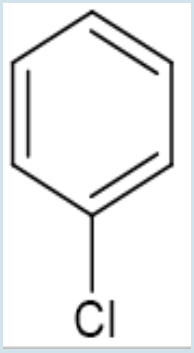	Cl	PS66	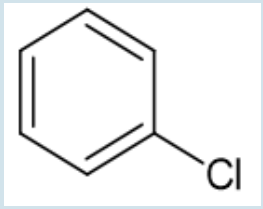	NO2

Figure 2: 3D Structure of monoamine oxidase (PDB ID: 2BXR).

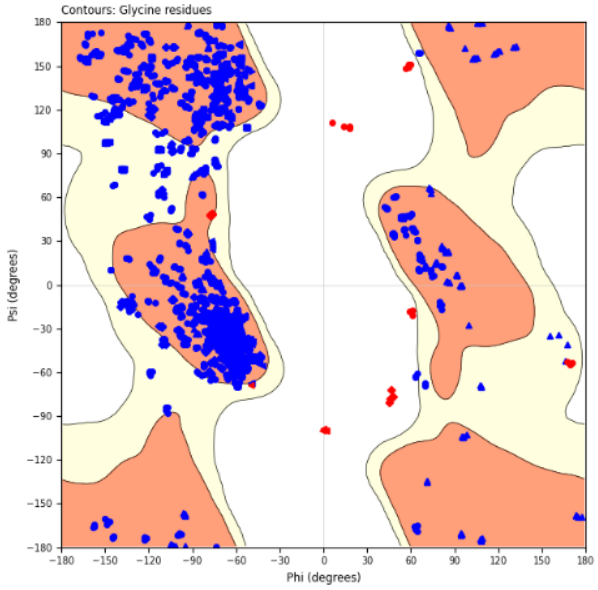

Figure 3: Ramachandran Plot.

ligand-protein interaction. The docking positions were evaluated in the extra-precision mode. The software recognizes hydrogen bonds, hydrophobic interactions, metal-ligation interactions, and steric conflicts. Every material has a molecular weight that is less than 500, ranging from 400 to 500. The calculated log P values of the compounds range from 3.56 to 5.35. The materials under investigation contain hydrogen bond donors.

SILICO ADMET

Quantum approaches are used in molecular modelling to assess the likelihood of interactions, such as those involving cytochrome P450, that are involved in ADME processes. Data modeling frequently uses QSAR techniques. These employ statistical techniques to find correlations in a group of structural molecules, such as GI absorption, BBB penetration, P-glycoprotein protein, CYP1A2 inhibitor, CYP2C9 inhibitor, CYP2D6 inhibitor, and CYP3A4 inhibitor, and specific properties. Models for effective prediction of the ADMET parameters require the selection of a suitable mathematical approach, the use of suitable chemical descriptors for the ADMET endpoint, and a sufficiently large collection of data related to the same endpoint for model validation. Effective property prediction methods are becoming more important to accomplish two primary objectives. First, novel compound libraries should be created to reduce the risk. Second, the most promising compounds should be the focus of screening and testing. Predicting. The goal of this study is to find features that provide information regarding dosage quantity and frequency, such as bioavailability, oral absorption, clearance, BBB penetration, and Vd (for frequency). Two sorts of computational

Table 2: Chemical interactions between the Chemicals and the Residues of Active Amino acids.

Compound Code	Active amino acid	Bond type	Docking score	2D	3D
PS1	ASP141 GLU458 TRP144 LEU460 TYR35 ARG454 ARG457	Conventional Hydrogen Bond Pi-Anion Pi-Pi T-shaped Alkyl Pi-Alkyl Pi-Alkyl Pi-Alkyl	-10.1	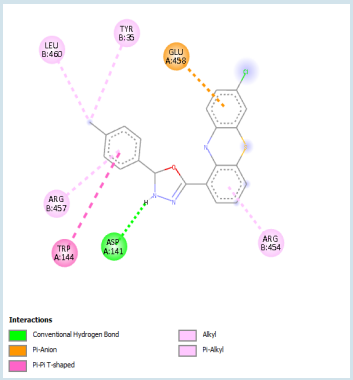	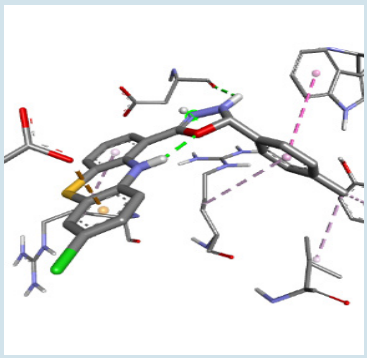
PS2	ASP141 ARG457 GLU458 ASN461 TRP144 LEU460 TYR35 ARG454 ARG457	Conventional Hydrogen Bond Carbon Hydrogen Bond Pi-Anion Pi-Donor Hydrogen Bond Pi-Pi T-shaped Alkyl Pi-Alkyl Pi-Alkyl Pi-Alkyl	-10.1	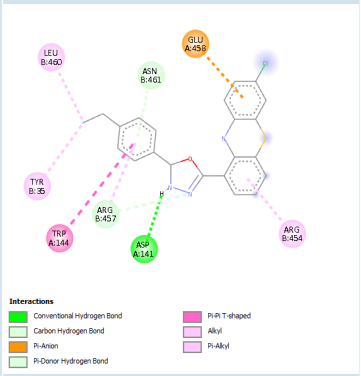	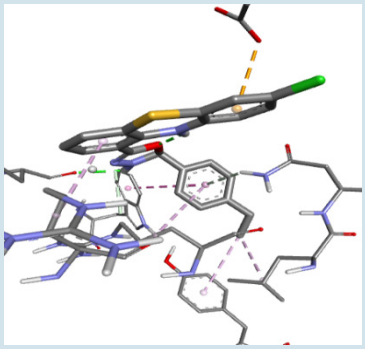
PS3	GLN425 GLU458 ASN461 ARG457	Conventional Hydrogen Bond Pi-Anion Pi-Donor Hydrogen Bond Pi-Alkyl	-9.9	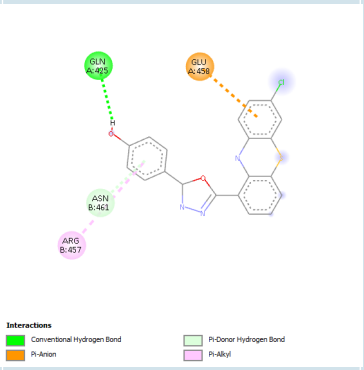	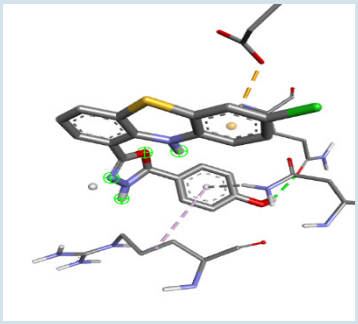

PS4	GLU216 GLU216 CYS406 TYR407 TRP441 TYR69 GLY66 PRO72 VAL303 LYS305 CYS406 PHE352 TRP397 TRP441	Pi-Anion Pi-Anion Pi-Sulfur Pi-Pi Stacked Pi-Pi Stacked Pi-Pi T-shaped Amide-Pi Stacked Alkyl Alkyl Alkyl Alkyl Pi-Alkyl Pi-Alkyl Pi-Alkyl	-11.3	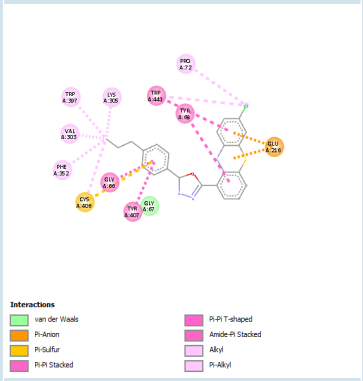	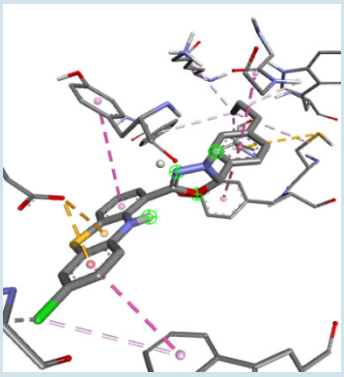
PS5	SER209 GLU216 PHE208 PHE208 TYR407 TYR444 ARG51 LEU97 CYS323 LEU337 ARG51 MET445 ILE335 LEU337	Conventional Hydrogen Bond Pi-Anion Pi-Pi Stacked Pi-Pi Stacked Pi-Pi Stacked Pi-Pi T-shaped Alkyl Alkyl Alkyl Alkyl Alkyl Pi-Alkyl Pi-Alkyl	-10	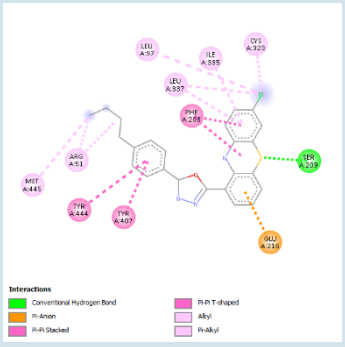	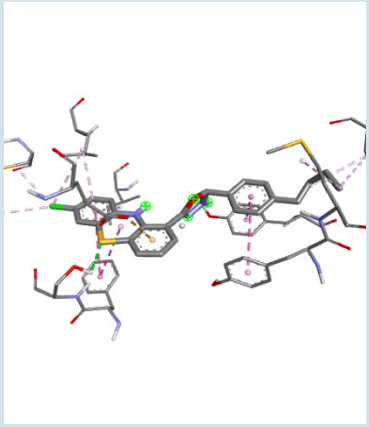

PS6	ASP141 GLN425 ARG457 GLU458 ASN461 TRP144 ARG457	Conventional Hydrogen Bond Conventional Hydrogen Bond Carbon Hydrogen Bond Pi-Anion Pi-Donor Hydrogen Bond Pi-Pi T-shaped Pi-Alkyl	-10.1	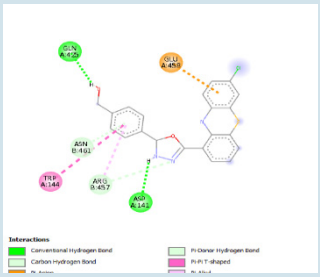	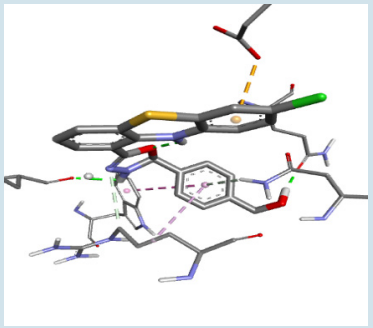
PS7	ARG457 ARG424 GLU458 ASN461 GLU458 ARG457	Conventional Hydrogen Bond Conventional Hydrogen Bond Conventional Hydrogen Bond Pi-Donor Hydrogen Bond Pi-Sigma Pi-Alkyl	-9.8	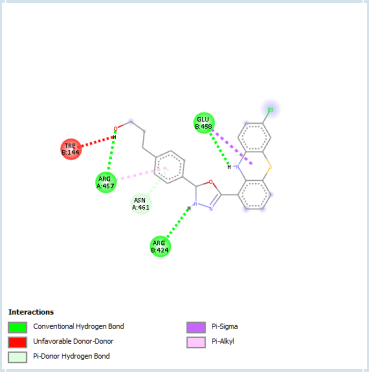	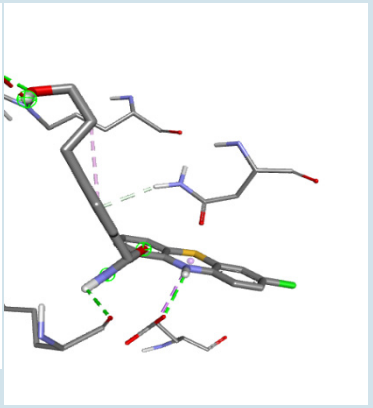
PS8	LEU277 TYR402 LYS280 ALA44 ILE273 TYR402 HIS282 LYS280 LYS280 LEU277	Conventional Hydrogen Bond Carbon Hydrogen Bond Pi-Cation Pi-Sigma Pi-Sigma Pi-Pi T-shaped Pi-Alkyl Pi-Alkyl Pi-Alkyl Pi-Alkyl	-10.5	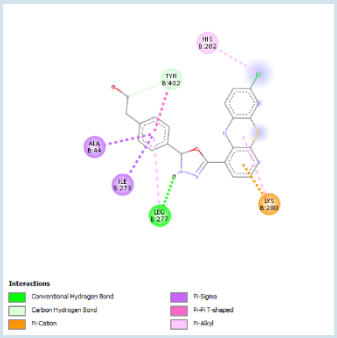	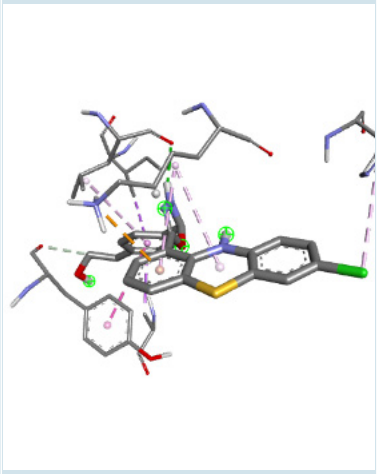

PS9	THR439 THR439 LYS440 LYS440 LYS440 LYS199 LYS440 LYS440 LYS440	Conventional Hydrogen Bond Sulfur-X Pi-Cation Pi-Sigma Pi-Sigma Alkyl Pi-Alkyl Pi-Alkyl Pi-Alkyl	-8.7	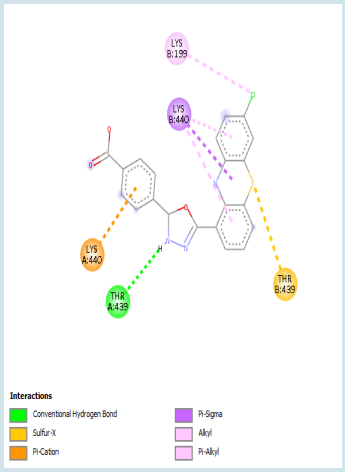	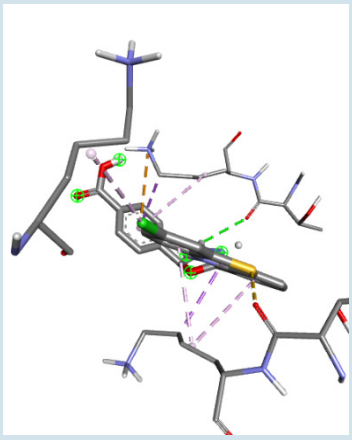
PS10	ARG424 ASP141 GLU458 ARG454 ARG457 ARG457 LEU460	Conventional Hydrogen Bond Conventional Hydrogen Bond Pi-Anion Pi-Alkyl Pi-Alkyl Pi-Alkyl Pi-Alkyl	-10.3	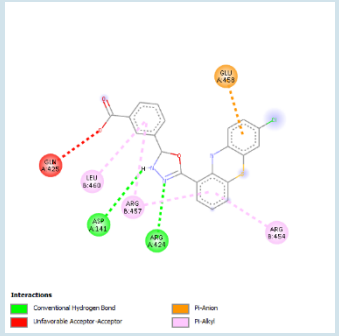	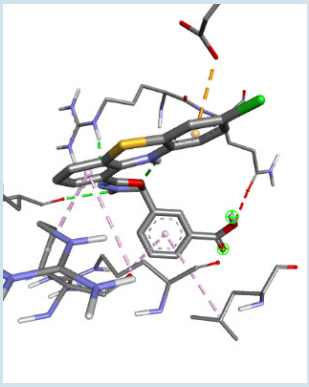
PS11	ARG424 PRO426 GLU458 GLU458 GLU458 ARG424 PRO426 ARG424	Conventional Hydrogen Bond Carbon Hydrogen Bond Pi-Anion Pi-Anion Pi-Anion Alkyl Pi-Alkyl Pi-Alkyl	-10.1	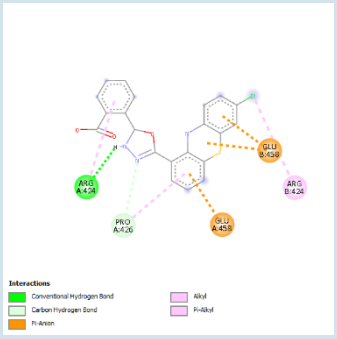	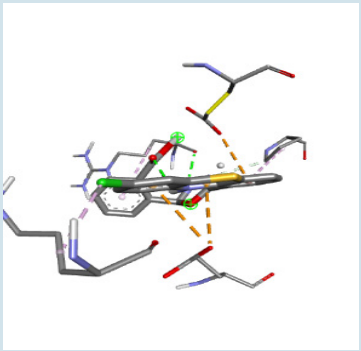

PS12	ALA68 SER209 GLU216 ILE335 LEU337 PHE208 PHE208 TYR407 TYR444 LEU97 CYS323 LEU337	Conventional Hydrogen Bond Sulfur-X Pi-Anion Pi-Sigma Pi-Sigma Pi-Pi Stacked Pi-Pi Stacked Pi-Pi Stacked Pi-Pi T-shaped Alkyl Alkyl Alkyl	-11.3	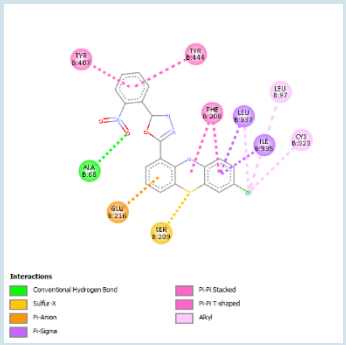	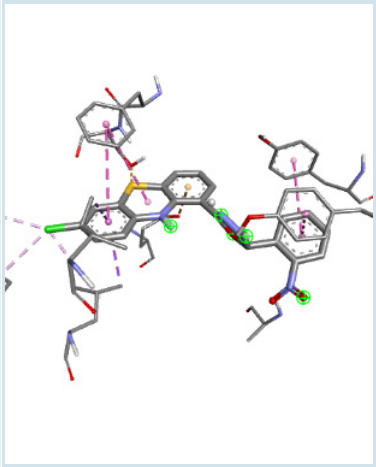
PS13	ASP141 GLU458 ASN461 TRP144 ARG457	Conventional Hydrogen Bond Pi-Anion Pi-Donor Hydrogen Bond Pi-Pi T-shaped Pi-Alkyl	-10.4	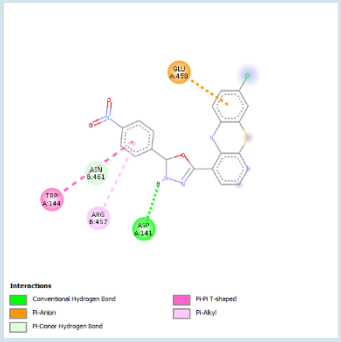	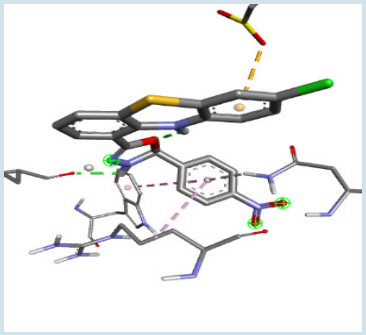
PS14	TRP144 TYR35 ASP141 ARG457 GLU458 ASN461 ARG454	Conventional Hydrogen Bond Conventional Hydrogen Bond Conventional Hydrogen Bond Carbon Hydrogen Bond Pi-Anion Pi-Donor Hydrogen Bond Pi-Alkyl	-10.5	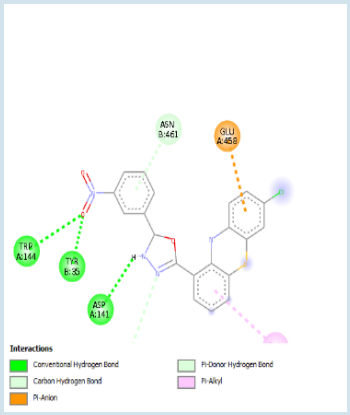	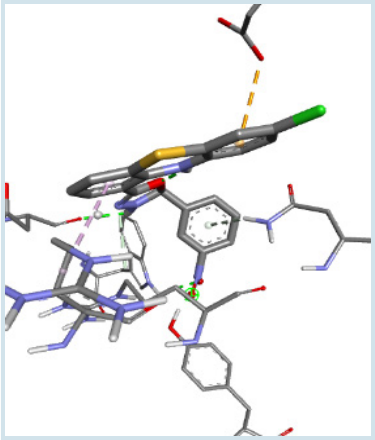

PS15	ASP141 GLU458 ASN461 ARG457	Conventional Hydrogen Bond Pi-Anion Pi-Donor Hydrogen Bond Pi-Alkyl	-10.0	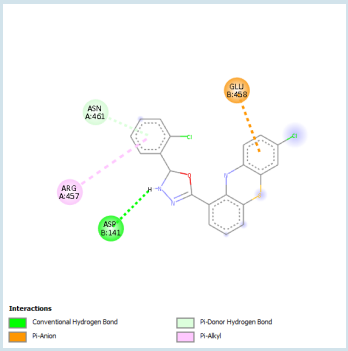	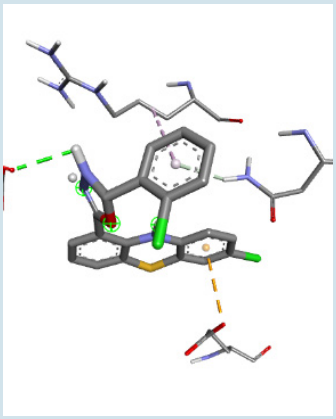
PS16	ASP141 GLU458 ASN461 LEU460 ARG457	Conventional Hydrogen Bond Pi-Anion Pi-Donor Hydrogen Bond Alkyl Pi-Alkyl	-10.0	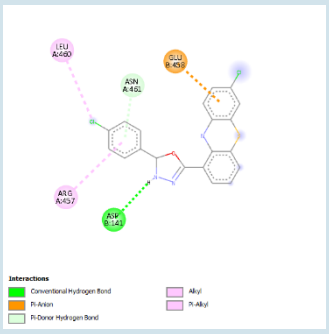	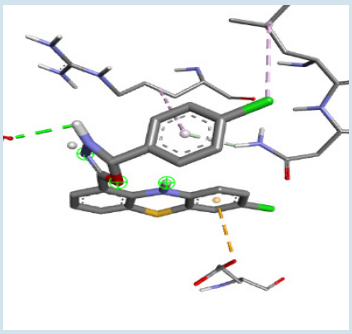
PS17	ASN461 ARG421 GLU458 ARG424 LEU460 ARG421 LEU460	Conventional Hydrogen Bond Conventional Hydrogen Bond Pi-Anion Pi-Donor Hydrogen Bond Alkyl Pi-Alkyl Pi-Alkyl	-10.3	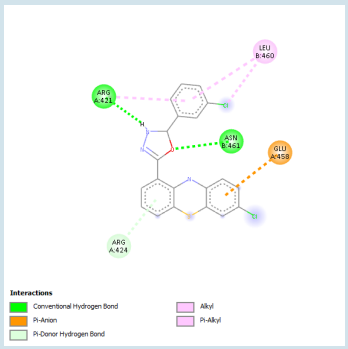	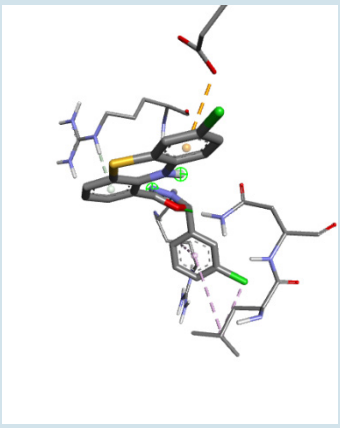

PS18	SER209 GLU216 CYS406 PHE208 3PHE208 TYR407 TYR444 LEU97 CYS323 LEU337 ILE335 LEU337 ARG51	Conventional Hydrogen Bond Pi-Anion Pi-Sulfur Pi-Pi Stacked Pi-Pi Stacked Pi-Pi Stacked Pi-Pi T-shaped Alkyl Alkyl Alkyl Pi-Alkyl Pi-Alkyl Pi-Alkyl	-12.3	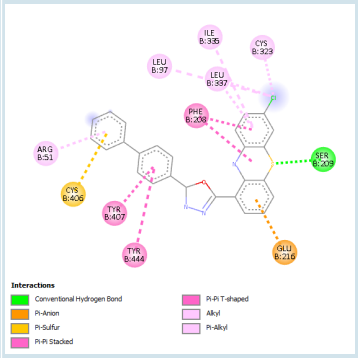	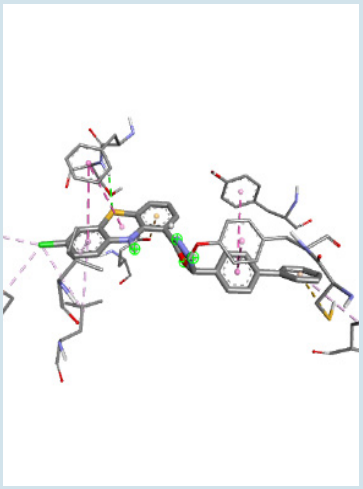
PS19	GLU216 ILE335 LEU337 PHE208 PHE208 TYR407 TYR444 CYS323 ILE335 LEU337	Pi-Anion Pi-Sigma Pi-Sigma Pi-Pi Stacked Pi-Pi Stacked Pi-Pi Stacked Pi-Pi T-shaped Alkyl Alkyl Alkyl	-11.1	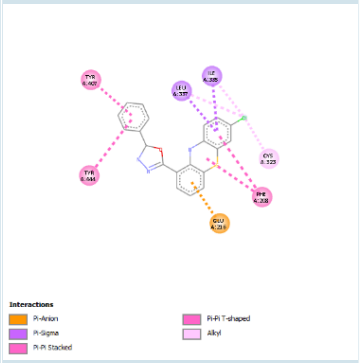	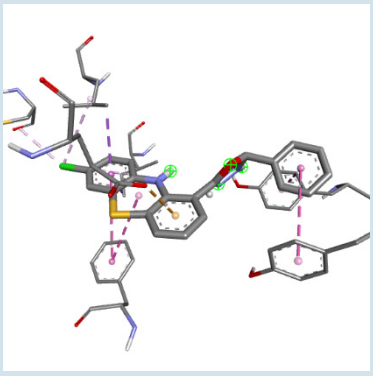

PS42	SER209 GLU216 ILE335 PHE208 PHE208 TYR407 TYR444 LEU97 CYS323 LEU337 LEU337	Conventional Hydrogen Bond Pi-Anion Pi-Sigma Pi-Pi Stacked Pi-Pi Stacked Pi-Pi Stacked Pi-Pi T-shaped Alkyl Alkyl Alkyl Pi-Alkyl	-11.1	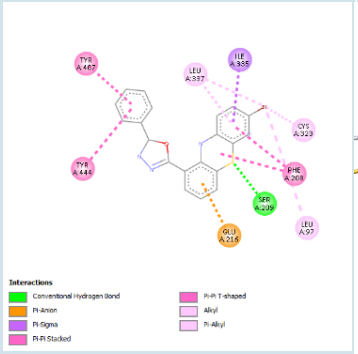	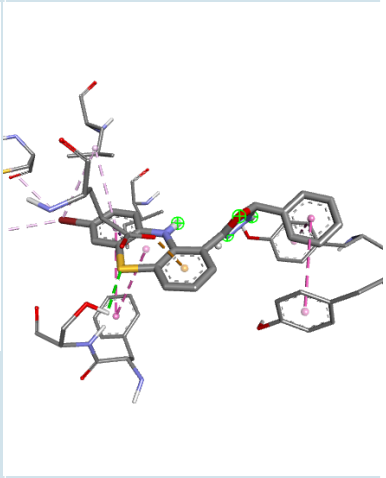
PS44	ARG424 ARG424 GLU458 ARG424 GLU458 PRO426 ARG424	Conventional Hydrogen Bond Conventional Hydrogen Bond Conventional Hydrogen Bond Pi-Donor Hydrogen Bond Pi-Sigma Pi-Alkyl Pi-Alkyl	-10.2	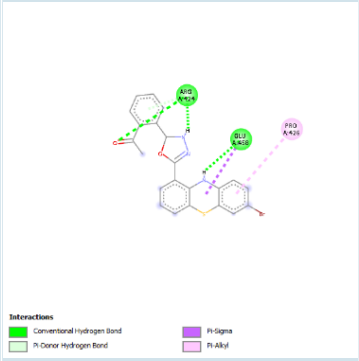	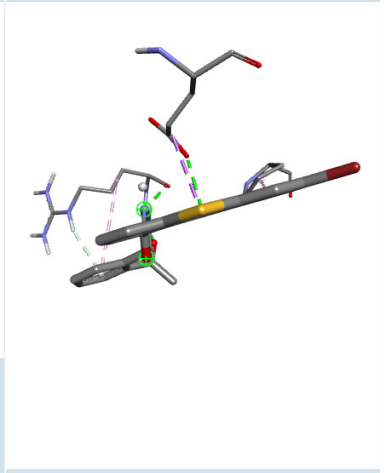
PS45	ASP141 ARG457 GLU458 ASN461 TRP144 ARG457	Conventional Hydrogen Bond Carbon Hydrogen Bond Pi-Anion Pi-Donor Hydrogen Bond Pi-Pi T-shaped Pi-Alkyl	-10.6	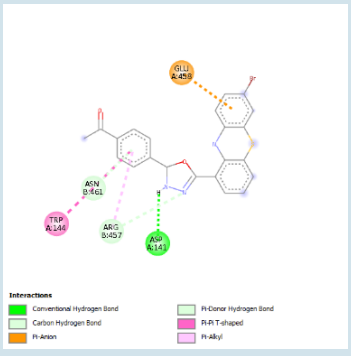	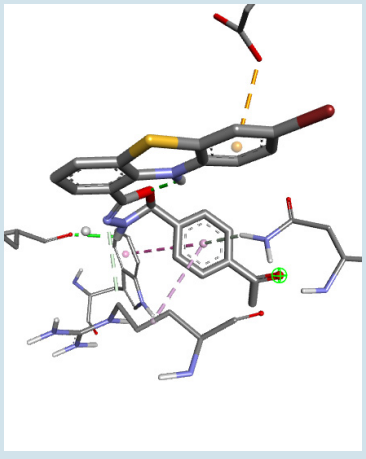

PS46	GLU216 ILE335 LEU337 PHE208 PHE208 TYR407 TYR444 CYS323 ILE335 LEU337	Pi-Anion Pi-Sigma Pi-Sigma Pi-Pi Stacked Pi-Pi Stacked Pi-Pi Stacked Pi-Pi T-shaped Alkyl Alkyl Alkyl	-12.0	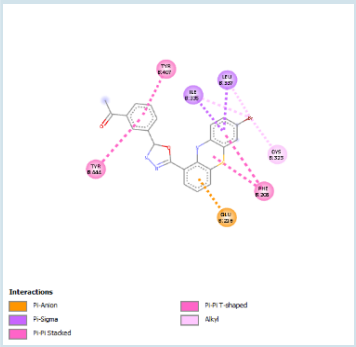	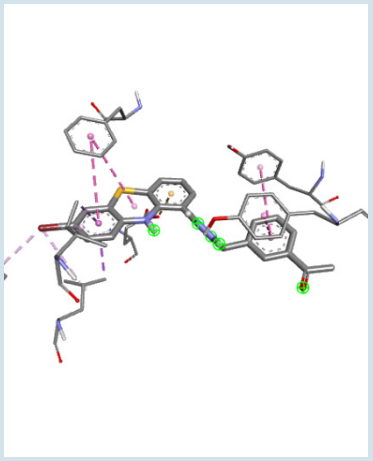
PS47	ARG76 ARG421 ASP141 LEU460 TYR35 ARG424 ARG457 ARG454 ARG457 LEU460	Conventional Hydrogen Bond Conventional Hydrogen Bond Pi-Anion Alkyl Pi-Alkyl Pi-Alkyl Pi-Alkyl Pi-Alkyl Pi-Alkyl Pi-Alkyl	-10.1	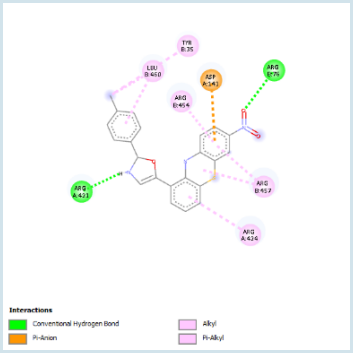	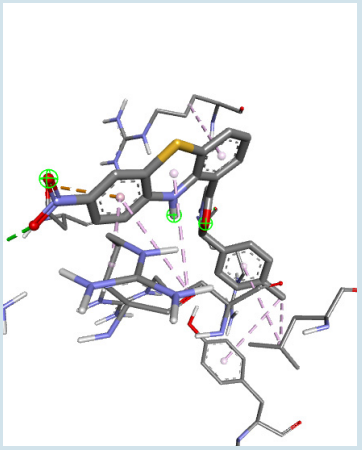
PS51	ASN461 ARG424 GLU145 ARG457 GLU458 ASN461 ARG457 ARG457 ARG424 ARG457	Conventional Hydrogen Bond Conventional Hydrogen Bond Conventional Hydrogen Bond Carbon Hydrogen Bond Pi-Anion Pi-Donor Hydrogen Bond Amide-Pi Stacked Pi-Alkyl Pi-Alkyl Pi-Alkyl	-9.8	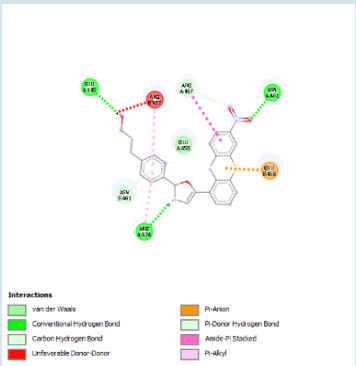	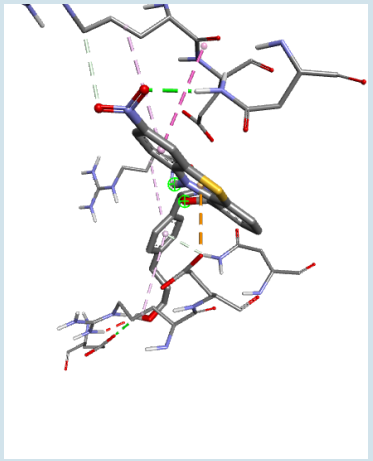

PS52	TYR35 ASN461 GLU145 GLU458 GLU458 ASN461 ARG454 ARG454 ARG457	Conventional Hydrogen Bond Conventional Hydrogen Bond Conventional Hydrogen Bond Carbon Hydrogen Bond Pi-Anion Pi-Donor Hydrogen Bond Pi-Alkyl Pi-Alkyl Pi-Alkyl	-9.6	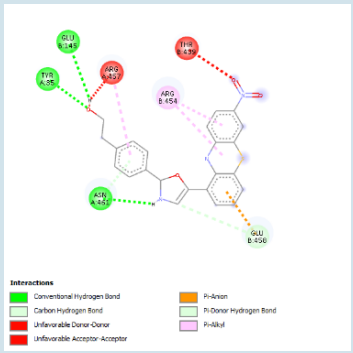	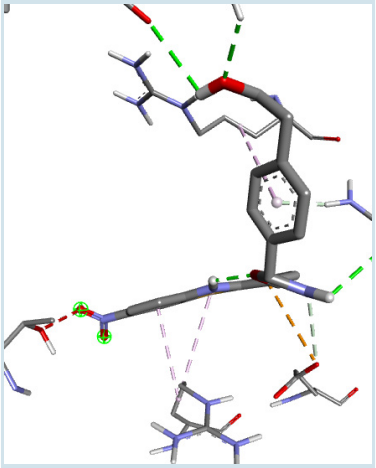
PS53	SER209 GLY71 GLU216 GLU216 CYS406 TYR407 TRP441 GLY66, GLY67	Conventional Hydrogen Bond Carbon Hydrogen Bond Pi-Anion Pi-Anion Pi-Sulfur Pi-Pi Stacked Pi-Pi Stacked Amide-Pi Stacked	-11.1	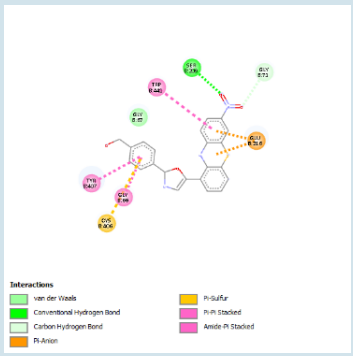	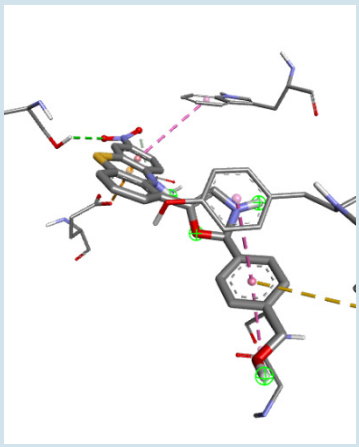
PS54	ARG424 ASN461 ASN461 GLU458 GLU458 GLU458 ARG424	Conventional Hydrogen Bond Conventional Hydrogen Bond Conventional Hydrogen Bond Pi-Anion Pi-Anion Pi-Anion Pi-Alkyl	-10.1	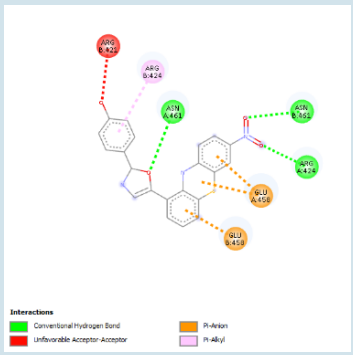	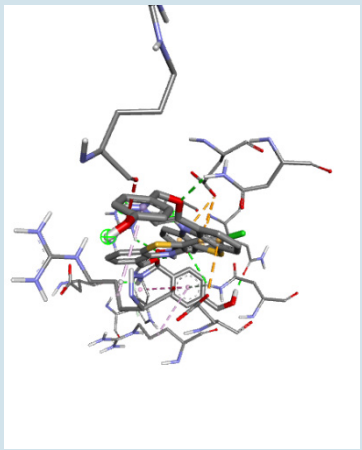

PS62	ARG421 ARG457 ASP141 LEU460 TYR35 ARG457 ARG424 ARG454 ARG457 ARG457 LEU460 ARG421	Conventional Hydrogen Bond Carbon Hydrogen Bond Pi-Anion Alkyl Pi-Alkyl Pi-Alkyl Pi-Alkyl Pi-Alkyl Pi-Alkyl Pi-Alkyl Pi-Alkyl Pi-Alkyl Pi-Alkyl	-9.8	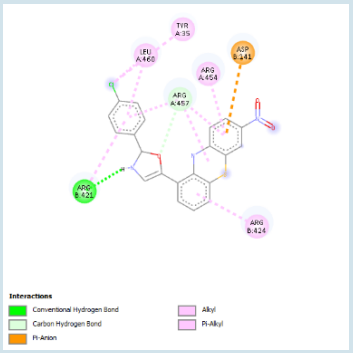	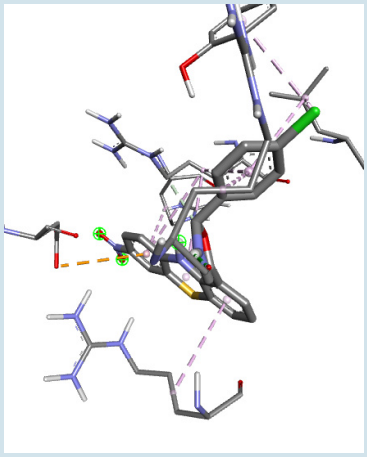
PS66	THR205 TRP128 TRP128 TYR121 TRP128 TRP128 TRP128 TRP128 TRP128 TRP128 TRP128 TYR121	Conventional Hydrogen Bond Pi-Sulfur Pi-Sulfur Pi-Pi Stacked Pi-Pi Stacked Pi-Pi Stacked Pi-Pi Stacked Pi-Pi Stacked Pi-Pi Stacked Pi-Pi Stacked Pi-Pi Stacked Pi-Alkyl	-10.0	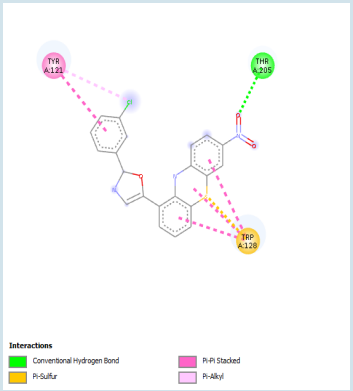	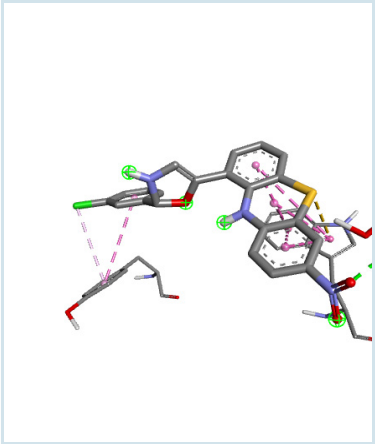

Table 3: Rotatable bonds; H-bond acceptors; H-bond donors; Lipinski violations; Ghose Violations; Veber Violations; Egan violations and Muegge violations of phenothiazine derivatives.

Compound. Code	Formula	Lipinski rule of five					Viber's rule	
		MW	iLOGP	#H-bond acceptors	#H-bond donors	Lipinski #violations	Rotatable bonds	TPSA
PS 1	$C_{21}H_{16}ClN_3OS$	393.89	3.65	2	2	1	2	70.95
PS 2	$C_{22}H_{18}ClN_3OS$	407.92	3.7	2	2	1	3	70.95
PS 3	$C_{20}H_{14}ClN_3O_2S$	395.86	2.98	3	3	1	2	91.18
PS 4	$C_{23}H_{20}ClN_3OS$	421.94	3.87	2	2	1	4	70.95
PS 5	$C_{24}H_{22}ClN_3OS$	435.97	3.88	2	2	1	5	70.95
PS 6	$C_{21}H_{16}ClN_3O_2S$	409.89	3.49	3	3	1	3	91.18
PS 7	$C_{23}H_{20}ClN_3O_2S$	437.94	3.34	3	3	1	5	91.18
PS 8	$C_{22}H_{18}ClN_3O_2S$	423.92	3.39	3	3	1	4	91.18
PS 9	$C_{21}H_{14}ClN_3O_3S$	423.87	2.65	4	3	1	3	108.25
PS 10	$C_{21}H_{14}ClN_3O_3S$	423.87	2.89	4	3	1	3	108.25
PS 11	$C_{21}H_{14}ClN_3O_3S$	423.87	2.8	4	3	1	3	108.25
PS 12	$C_{20}H_{13}ClN_4O_3S$	424.86	2.85	4	2	1	3	116.77
PS 13	$C_{20}H_{13}ClN_4O_3S$	424.86	2.7	4	2	1	3	116.77
PS 14	$C_{20}H_{13}ClN_4O_3S$	424.86	2.87	4	2	1	3	116.77
PS 15	$C_{20}H_{13}Cl_2N_3OS$	414.31	3.45	2	2	1	2	70.95
PS 16	$C_{20}H_{13}Cl_2N_3OS$	414.31	3.63	2	2	1	2	70.95
PS 17	$C_{20}H_{13}Cl_2N_3OS$	414.31	3.7	2	2	1	2	70.95
PS 18	$C_{26}H_{18}ClN_3OS$	455.96	3.73	2	2	1	3	70.95
PS 19	$C_{20}H_{14}ClN_3OS$	379.86	3.6	2	2	1	2	70.95
PS 20	$C_{26}H_{18}ClN_3OS$	455.96	3.77	2	2	1	3	70.95
PS 21	$C_{22}H_{16}ClN_3O_2S$	421.9	3.16	3	2	1	3	88.02
PS 22	$C_{22}H_{16}ClN_3O_2S$	421.9	3.32	3	2	1	3	88.02
PS 23	$C_{22}H_{16}ClN_3O_2S$	421.9	3.3	3	2	1	3	88.02
PS 24	$C_{21}H_{16}BrN_3OS$	438.34	3.85	2	2	1	2	70.95
PS 25	$C_{22}H_{18}BrN_3OS$	452.37	3.78	2	2	1	3	70.95
PS 26	$C_{20}H_{14}BrN_3O2S$	440.31	3	3	3	1	2	91.18
PS 27	$C_{23}H_{20}BrN_3OS$	466.39	4.03	2	2	1	4	70.95
PS 28	$C_{24}H_{22}BrN_3OS$	480.42	4.27	2	2	1	5	70.95
PS 29	$C_{21}H_{16}BrN_3O2S$	409.89	3.49	3	3	1	3	91.18
PS 30	$C_{23}H_{20}BrN_3O_2S$	482.39	3.55	3	3	1	5	91.18
PS 31	$C_{22}H_{18}BrN_3O_2S$	468.37	3.5	3	3	1	4	91.18
PS 32	$C_{21}H_{14}BrN_3O_3S$	468.32	2.93	4	3	1	3	108.25
PS 33	$C_{21}H_{14}BrN_3O_3S$	468.32	2.69	4	3	1	3	108.25
PS 34	$C_{21}H_{14}BrN_3O_3S$	468.32	2.69	4	3	1	3	108.25
PS 35	$C_{20}H_{13}BrN_4O_3S$	469.31	2.98	4	2	1	3	116.77
PS 36	$C_{20}H_{13}BrN_4O_3S$	469.31	2.8	4	2	1	3	116.77
PS 37	$C_{20}H_{13}BrN_4O_3S$	469.31	2.94	4	2	1	3	116.77
PS 38	$C_{20}H_{13}BrClN_3OS$	458.76	3.58	2	2	1	2	70.95
PS 39	$C_{20}H_{13}BrClN_3OS$	458.76	3.68	2	2	1	2	70.95
PS 40	$C_{20}H_{14}Br_2ClN_3OS$	539.67	0	2	2	2	2	70.95
PS 41	$C_{26}H_{19}Br_2N_3OS$	581.32	0	2	2	2	3	70.95

PS 42	$C_{20}H_{14}BrN_3OS$	424.31	3.71	2	2	1	2	70.95
PS 43	$C_{26}H_{18}BrN_3OS$	500.41	3.8	2	2	2	3	70.95
PS 44	$C_{22}H_{16}BrN_3O_2S$	466.35	3.27	3	2	1	3	88.02
PS 45	$C_{22}H_{16}BrN_3O2S$	466.35	3.38	3	2	1	3	88.02
PS 46	$C_{22}H_{16}BrN_3O2S$	466.35	3.39	3	2	1	3	88.02
PS 47	$C_{22}H_{17}N_3O_3S$	403.45	2.99	3	2	0	3	104.41
PS 48	$C_{23}H_{19}N_3O_3S$	417.48	3.24	3	2	1	4	104.41
PS 49	$C_{24}H_{21}N_3O_3S$	431.51	3.43	3	2	1	5	104.41
PS 50	$C_{25}H_{23}N_3O_3S$	445.53	3.83	3	2	1	6	104.41
PS 51	$C_{24}H_{21}N_3O_4S$	447.51	3.18	4	3	0	6	124.64
PS 52	$C_{23}H_{19}N_3O_4S$	433.48	3.02	4	3	0	5	124.64
PS 53	$C_{22}H_{17}N_3O_4S$	419.45	2.87	4	3	0	4	124.64
PS 54	$C_{21}H_{15}N_3O_4S$	405.43	2.16	4	3	0	3	124.64
PS 55	$C_{22}H_{15}N_3O_5S$	433.44	2.55	5	3	0	4	141.71
PS 56	$C_{22}H_{15}N_3O_5S$	433.44	2.26	5	3	0	4	141.71
PS 57	$C_{22}H_{15}N_3O_5S$	433.44	1.93	5	3	0	4	141.71
PS 58	$C_{21}H_{14}N_4O_5S$	434.42	2.55	5	2	0	4	150.23
PS 59	$C_{21}H_{14}N_4O_5S$	434.42	2.65	5	2	0	4	150.23
PS 60	$C_{21}H_{14}N_4O_5S$	434.42	2.58	5	2	0	4	150.23
PS 61	$C_{21}H_{14}C_lN_3O_3S$	423.87	2.98	3	2	1	3	104.41
PS 62	$C_{21}H_{14}C_lN_3O_3S$	423.87	2.9	3	2	1	3	104.41
PS63	$C_{23}H_{17}N_3O_4S$	431.46	2.9	4	2	0	4	121.48
PS 64	$C_{23}H_{17}N_3O_4S$	431.46	2.7	4	2	0	4	121.48
PS 65	$C_{23}H_{17}N_3O_4S$	431.46	2.66	4	2	0	4	121.48
PS 66	$C_{21}H_{14}C_lN_3O_3S$	423.87	2.77	3	2	1	3	104.41

Table 4: *In silico* ADMET of Phenothiazine derivatives.

Comp code	GI absorption	BBB permeant	Pgp substrate	CYP1A2 inhibitor	CYP2C19 inhibitor	CYP2C9 inhibitor	CYP2D6 inhibitor	CYP3A4 inhibitor	Lipinski #violations	Bioavailability Score
PS 1	High	Yes	Yes	Yes	Yes	Yes	No	Yes	1	0.55
PS 2	High	Yes	Yes	Yes	Yes	Yes	No	Yes	1	0.55
PS 3	High	No	No	No	Yes	Yes	No	Yes	1	0.55
PS 4	High	No	Yes	Yes	Yes	Yes	Yes	Yes	1	0.55
PS 5	High	No	Yes	Yes	Yes	Yes	Yes	Yes	1	0.55
PS 6	High	No	Yes	Yes	Yes	Yes	Yes	Yes	1	0.55
PS 7	High	No	Yes	Yes	Yes	Yes	Yes	Yes	1	0.55
PS 8	High	No	Yes	Yes	Yes	Yes	Yes	Yes	1	0.55
PS 9	High	No	No	No	No	Yes	No	No	1	0.56
PS 10	High	No	No	No	No	Yes	No	No	1	0.56
PS 11	High	No	No	No	No	Yes	No	No	1	0.56
PS 12	High	No	No	No	Yes	Yes	No	No	1	0.55
PS 13	High	No	No	No	Yes	Yes	No	No	1	0.55
PS 14	High	No	No	No	Yes	Yes	No	No	1	0.55
PS 15	High	Yes	Yes	Yes	Yes	Yes	No	No	1	0.55
PS 16	High	Yes	Yes	Yes	Yes	Yes	No	No	1	0.55
PS 17	High	Yes	No	Yes	Yes	Yes	No	No	1	0.55
PS 18	High	No	No	Yes	Yes	Yes	No	No	1	0.55
PS 19	High	Yes	No	Yes	Yes	Yes	No	Yes	1	0.55

PS 20	High	No	No	Yes	Yes	Yes	No	No	1	0.55
PS 21	High	No	No	No	Yes	Yes	No	Yes	1	0.55
PS 22	High	No	No	Yes	Yes	Yes	No	Yes	1	0.55
PS 23	High	No	No	Yes	Yes	Yes	No	Yes	1	0.55
PS 24	High	Yes	Yes	Yes	Yes	Yes	No	No	1	0.55
PS 25	High	Yes	Yes	Yes	Yes	Yes	No	Yes	1	0.55
PS 26	High	No	No	No	No	Yes	No	Yes	1	0.55
PS 27	High	No	Yes	Yes	Yes	Yes	Yes	Yes	1	0.55
PS 28	High	No	Yes	Yes	No	Yes	Yes	Yes	1	0.55
PS 29	High	No	Yes	Yes	Yes	Yes	Yes	Yes	1	0.55
PS 30	High	No	Yes	Yes	No	Yes	Yes	Yes	1	0.55
PS 31	High	No	Yes	Yes	No	Yes	Yes	Yes	1	0.55
PS 32	High	No	No	No	No	Yes	No	No	1	0.56
PS 33	High	No	No	No	No	Yes	No	No	1	0.56
PS 34	High	No	No	No	No	Yes	No	No	1	0.56
PS 35	High	No	No	No	Yes	Yes	No	No	1	0.55
PS 36	High	No	No	No	Yes	Yes	No	No	1	0.55
PS 37	High	No	No	No	Yes	Yes	No	No	1	0.55
PS 38	High	No	No	Yes	Yes	Yes	No	No	1	0.55
PS 39	High	No	No	Yes	Yes	Yes	No	No	1	0.55
PS 40	High	No	Yes	Yes	No	No	No	No	2	0.17
PS 41	Low	No	Yes	Yes	Yes	No	No	No	2	0.17
PS 42	High	Yes	No	Yes	Yes	Yes	No	Yes	1	0.55
PS 43	High	No	No	Yes	Yes	No	No	No	2	0.17
PS 44	High	No	No	Yes	Yes	Yes	No	Yes	1	0.55
PS 45	High	No	No	Yes	Yes	Yes	No	Yes	1	0.55
PS 46	High	No	No	Yes	Yes	Yes	No	Yes	1	0.55
PS 47	High	No	Yes	Yes	Yes	Yes	No	Yes	0	0.55
PS 48	High	No	No	Yes	Yes	Yes	No	Yes	1	0.55
PS 49	High	No	No	Yes	Yes	Yes	No	Yes	1	0.55
PS 50	Low	No	Yes	Yes	Yes	Yes	Yes	Yes	1	0.55
PS 51	Low	No	Yes	Yes	Yes	Yes	Yes	Yes	0	0.55
PS 52	High	No	Yes	Yes	Yes	Yes	Yes	Yes	0	0.55
PS 53	High	No	Yes	Yes	Yes	Yes	No	Yes	0	0.55
PS 54	High	No	Yes	Yes	Yes	Yes	No	Yes	0	0.55
PS 55	Low	No	No	Yes	Yes	Yes	No	No	0	0.56
PS 56	Low	No	No	Yes	Yes	Yes	No	No	0	0.56
PS 57	Low	No	No	Yes	Yes	Yes	No	No	0	0.56
PS 58	Low	No	No	Yes	Yes	Yes	No	Yes	0	0.55
PS 59	Low	No	No	No	Yes	Yes	No	No	0	0.55
PS 60	Low	No	No	Yes	Yes	Yes	No	Yes	0	0.55
PS 61	High	No	No	Yes	Yes	Yes	No	Yes	1	0.55
PS 62	High	No	No	Yes	Yes	Yes	No	Yes	1	0.55
PS63	Low	No	No	Yes	Yes	Yes	No	Yes	0	0.55
PS 64	Low	No	No	Yes	Yes	Yes	No	Yes	0	0.55
PS 65	Low	No	No	Yes	Yes	Yes	No	Yes	0	0.55
PS 66	High	No	No	Yes	Yes	Yes	No	Yes	1	0.55

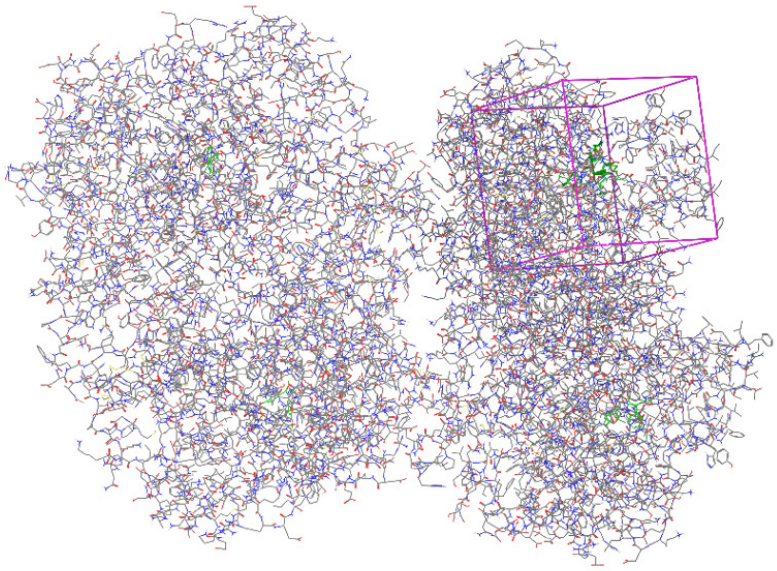

Figure 4: Receptor Grid Generation Wizard.

approaches are used: data modelling and molecular modelling. This article examines recent advances in the prediction of physicochemical properties relevant to ADME features (like absorption), and toxicity issues see Table 4. The use of automated medium and HTS in vitro tests will increase throughout the next 10 or more years.

DISCUSSION

The optimal conformation gets determined by analogs is the good interactions and Auto dock values that are close to zero. The Ramachandran and RMSD plot analyses of both complexes indicated that the PS9-protein complex maintained a stable trajectory, demonstrating excellent stability after 100 ns, suggesting its suitability for further studies. Analysis of the synthetic phenothiazine derivatives showed that all the compounds had molecular weights below 500, showing that they have an action site binding effect. A favourable in vivo reaction requires a balance between pharmacodynamics and pharmacokinetic parameters. Additionally, ADMET provides additional information on medication dosage and regimen. In accordance with an oral medication is selected according to Lipinski's "rule of five" if its log P value is less than five, its molecular weight is less than 500, and its hydrogen bond donors and acceptors are fewer than five and ten, respectively. Rotatable bond count indicates molecular flexibility, which is essential for oral bioavailability. Given its indirect relationship to percentage absorption, it was also proposed that TPSA be used as a 3D descriptor of the quantity of hydrogen bonding groups. Each drug had a Log P value less than 5, showing better absorption and penetration of cell membranes. The "binding energies and hydrogen bonds" of PS1-PS16 are detailed for several phenothiazine derivatives in Table 1. Furthermore, TPSA was suggested as a 3D descriptor for the number of hydrogen bonding groups due to its indirect relationship to percentage absorption. A Log P value less than five signified that each medication had superior cell membrane penetration and absorption. Table 1 lists the various phenothiazine derivatives along with information on the "binding energies and hydrogen bonds" of "PS1-PS16. Phe381, Leu-384, Tyr-385, Trp-387, Phe-518, Gly-526, Met-522, Tyr348, Val-349, Leu-352 Monoamine included active amino acids. oxidase (PDB ID: 2BXR) Enzyme: PS5 and PS6 demonstrated Pi-Pi stacking to TYR355: HH; SER 530: HG; SER530: HB1; TYR355; PHE381; TYR385; TRP387; TRP387; TRP387; ALA527: N; LEU384; MET522; VAL349; ALA527; and LEU531 across the phenothiazine and form an H-bond with Ser-530 through the phenothiazine ring's nitrogen. PPS15 displayed Pi-Pi stacking with Tyr385 across the phenothiazine ring and H-bonding with Ser530. With ARG120: HH11; ARG120: HH12; TYR 355: HH; ARG120: NH1; ARG120: NH2; VAL89; VAL116; VAL349; ALA527; VAL349 and LEU352; ALA527 via benzene ring and H-bond with Met-522 through nitrogen, PS11 showed Pi-Pi stacking. Comparing the 16 phenothiazine derivatives to the standard Indomethacin (-10.705 kcal/mol), a respectable" docking score of -8.572 kcal/mol was found for PS15 and PS11. VAL 89, VAL116, VAL349, ALA527, VAL349, LEU352, "ARG120:HH11; ARG120:HH12; TYR355: HH; ARG120:NH1; ARG120:NH2. There were active amino acids in the monoamine oxidase enzyme. PDB ID: 2BXR Enzyme: enzymes. PS5 proposed an H-Bond with TYR355: HH; SER 530: HG; SER530: HB1; TYR355; PHE381; TYR385; TRP387; TRP387; TRP387; ALA527: N; LEU384; MET522; VAL349; ALA527; and LEU531 nitrogen of phenothiazine and Pi-Pi stacking with Tyr-385 via benzene for PS5. TYR 355: HH; SER530: HG; SER530: HB1; PHE381; TYR385; TRP387; TRP387; TRP387; VAL116; LEU359; LEU531; LEU384; MET522; VAL349; ALA;527 and LEU531 via phenothiazine and Pi-pi stacking with Tyr-385 and Trp-387 by benzene were identified by PS13.

H-bond with ARG120:HH12, ARG120:NH1, LEU93, VAL116, VAL349, ALA527, LEU352, and Ser-530 was" demonstrated by PS9 through phenothiazine and Pi-Pi stacking with Tyr-385. When compared to the conventional Indomethacin (-10.099 kcal/mol), 16 phenothiazine derivatives, PS5, PS6, PS11, PS13, and PS15 displayed higher "docking scores ranging from -8.25 to -8.51 kcal/mol. The binding affinity score of compound PS5 with COX-1 (PDB: 3KK6) is -56.79 kcal/mol, while compound PS6 has a binding affinity score of -60.27 kcal/mol with MONOAMINE OXIDASE (PDB ID: 2BXR) (PDB: 3LN1). High ADME was also indicated by the compounds' oral absorption percentage, which varied from 70.69 to 73.87%. Rotatable bonds ranged from 7 to 8 (<10), and their respective TPSA values were 101.3 and 104.80 A2 (140 A2). It is often believed that a molecule has both lipophilicity and hydrophilicity if it is soluble in water and meets Lipinski's requirements. The enzymes' interactions with the monoamine oxidase (PDB ID: 2BXR) enzyme demonstrated their anti-depressant activity. TYR355: HH; SER530: HG; SER530: HB1; TYR355; PHE381; TYR385; TRP387; TRP387; TRP387; ALA527: N; LEU384; MET522; VAL349; ALA527; and LEU531 were monoamine oxidase's active amino acids (PDB ID: 2BXR). Enzyme: PS13 and PS15 showed that they could form an H-bond with Ser-530 through the nitrogen of the phenothiazine ring and Pi-Pi stack to Tyr385 and Trp387 via the phenothiazin.PS12 showed Pi-Pi stacking with TYR355: HH; SER530: HG; SER530: HB1; TYR355; PHE381; TYR385; TRP387; TRP387; TRP387; ALA527: N; VAL349; ALA527; and LEU531 by hydrogen bonding with Ser530 and the phenothiazin ring. PS14 showed that it could form an H-bond with Met-522 through nitrogen and Pi-Pi stacking with Tyr-385 through the benzene ring. The 16 phenothiazin derivatives had a respectable docking score of -8.572kcal/mol" when compared to the standard Indomethacin (-10.705 kcal/mol). The monoamine oxidase enzyme was active for the amino acids Phe381, Leu384, Tyr385, and Trp387 (PDB ID: 2BXR). The enzyme is the enzyme. H-Bond with Ser-530 nitrogen of phenothiazine and Pi-Pi stacking with Tyr-385 via benzene were demonstrated by BI5. TYR355: HH; SER530: HG; SER530: HB1; TYR355; PHE381; TYR385; TRP387; TRP387; TRP387; ALA527: N; LEU384; MET522; VAL349; ALA527; and LEU531 were shown to exhibit Pi-cation interaction through phenothiazine and Pi-pi stacking with Tyr-385 and Trp-387 via benzene. TYR355: HH; SER530: HG; SER530: HB1; TYR355; PHE381; TYR385; TRP387; TRP387; TRP387; ALA527: N; LEU384; MET522; VAL349; ALA527; and LEU531 were shown to form an H-bond with PS1 by phenothiazine and Pi-Pi stacking with Tyr-385.A balanced combination of pharmacodynamics and pharmacokinetic properties is necessary for a favourable reaction in vivo. ADMET also provides more information on medication dosage and regimen.

CONCLUSION

Among the 16 phenothiazine derivatives, the ligands PS15 and PS13 displayed high docking scores with the enzymes COX-1 (PDB: 3KK6) (-9.492 kcal/mol) and monoamine oxidase (PDB ID: 2BXR) (PDB: 3LN1) (-8.572 kcal/mol), respectively. Also revealed were the pharmacophores properties that support their biological function. The binding and affinity between the monoamine oxidase (PDB ID: 2BXR) enzyme and phenothiazine, which are responsible for the antidepressant activity features, have thus been identified with the use of these in silico techniques. We docked phenothiazine analogues with monoamine oxidase (PDB ID: 2BXR) enzymes to determine their anti-depressant activity features. It was found that the values of all the compounds fell within usual range, and Lipinski's rule of five wasn't violated. This means that the chemicals are expected to have a high oral bioavailability.

ACKNOWLEDGEMENT

The authors are thankful to Pravara Rural College of Pharmacy, Pravaranagar.

ABBREVIATIONS

ADME: Absorption, Distribution, Metabolism, and Excretion; **BBB:** Blood-Brain Barrier; **CNS:** Central Nervous System; **CYP:** CytochromeP450**; CYP1A2:** Cytochrome P450 1A2; **CYP2C19:** Cytochrome P450 2C19; **CYP2C9:** Cytochrome P450 2C9; **CYP2D6:** Cytochrome P450 2D6; **CYP3A4:** Cytochrome P450 3A4; **GI:** Gastrointestinal; **HBA:** Hydrogen Bond Acceptor; **HBD:** Hydrogen Bond Donor; **Log Kp:** Logarithm of Skin Permeation Coefficient; **LogP:** Logarithm of Octanol: Water Partition Coefficient; **MW:** Molecular Weight; **PSA:** Polar Surface Area; **SA Score:** Synthetic Accessibility Score.

CONFLICT OF INTEREST

The authors declare that there is no conflict of interest.

AUTHORS CONTRIBUTIONS

Sanket Keshav Tambe: *In silico* ADMET (Absorption, Distribution, Metabolism, Excretion). Rohit Jaysing Bhor: In silico ADMET (Absorption, Distribution, Metabolism, Excretion). Sagar Dattatray Magar: SWISS ADMET Software Data. Mayur Shivaji Bhosale: SWISS ADMET Software Data. Shubham Popatrao Mankar: Docking images of 2D and 3D by Discovery Studio 2021. Datta Macchindra Abhale: Docking images of 2D and 3D by Discovery Studio 2021. Sachin Tukaram Chavan: Research drafting. Gaurav Subhash Damre: Research drafting.

REFERENCES

A.F.S. Barbosa, I.P. Santos, G.M.P. Santos, T.M. Bastos, Rocha, P.C. Vinícius, et al. (2020) Anti-Trypanosoma cruzi effect of the photodynamic antiparasitic chemotherapy using phenothiazine derivatives as photosensitizers. Lasers Med. Sci., 35 (1) 79-85

B.A. Babalola, A.E. Adegboyega (2024). Computational discovery of novel imidazole derivatives as inhibitors of SARS-CoV-2 main protease: an integrated approach combining molecular dynamics and binding affinity analysis. COVID, 4(6), 672-695,

B.A. Babalola, A.I. Akinwande, A.A. Otunba, G.E. Adebami, O. Babalola, C. Nwufo. (2014). Therapeutic benefits of Carica papaya: a review on its pharmacological activities and characterization of papain. Arab. J. Chem., 17 (1)

B.A. Babalola, A.I. Akinwande, A.E. Gboyega, A.A. Otunba (2023) Extraction, purification and characterization of papain cysteine-proteases from the leaves of Carica papaya. Scientific African, 19, e01538

B.A. Babalola, G.E. Adebami, S.E. Akinsuyi (2021). Mechanistic basis for cancer immune evasion and role of immune checkpoint blockades in immuno-oncology, Global J. Cancer Ther., 7(1), 035-042

B.A. Babalola, T.E. Adetobi, O.S. Akinsuyi, O.A. Adebisi, E.O. Folajimi, (2021) Computational study of the therapeutic potential of novel heterocyclic derivatives against SARS-CoV-2. Covid, 1(4), 757-774

Ben-Levy, R., Hooper, S., Wilson, R., Paterson, H. F., & Marshall, C. J. (1998). Nuclear export of the stress-activated protein kinase p38 mediated by its substrate MAPKAP kinase-2. Current Biology, 8(19), 1049-1057. https://doi.org/10.1016/s0960-9822(98)70442-7

Boehm, J. C., Smietana, J. M., Sorenson, M. E., Garigipati, R. S., Gallagher, T. F., Sheldrake, P. L., Bradbeer, J., Badger, A. M., Laydon, J. T., Lee, J. C., Hillegass, L. M., GriPSold, D. E., Breton, J. J., Chabot-Fletcher, M. C., & Adams, J. L. (1996). 1-Substituted 4-Aryl-5-pyridinylimidazoles: A new class of cytokine suppressive drugs with low 5-lipoxygenase and monoamine oxidase (PDB ID: 2BXR) enzyme: Inhibitory potency. Journal of Medicinal Chemistry, 39(20), 3929-3937. https://doi.org/10.1021/jm960415o

C. Gopi, M.D. Dhanaraju (2019) Recent progress in synthesis, structure and biological activities of phenothiazine derivatives. Rev. J. Chem., 9, 95-126

Chan, W., Almasieh, M., Catrinescu, M., & Levin, L. A. (2017). Cobalamin-associated superoxide scavenging in neuronal cells is a potential mechanism for vitamin B12-deprivation optic neuropathy. American Journal of Pathology, 188(1), 160-172. https://doi.org/10.1016/j.ajpath.2017.08.032

Cuadrado, A., & Nebreda, A. R. (2010). Mechanisms and functions of p38 MAPK signalling. Biochemical Journal, 429(3), 403-417. https://doi.org/10.1042/bj20100323

E.T. Adetobi, S.O. Akinsuyi, O.A. Ahmed, E.O. Folajimi, B.A. Babalola (2022). In silico evaluation of the inhibitory potential of cymbopogonol from Cymbopogon citratus towards falcipain-2 (FP2) cysteine protease of Plasmodium falciparum. Trop. J. Nat. Product Res., 6 (10) [2]

F.J. Femi-Olabisi, A.A. Ishola, O. Faokunla, A.O. Agboola, B.A. Babalola (2021). Evaluation of the inhibitory potentials of selected compounds from Costus spicatus (Jacq.) rhizome towards enzymes associated with insulin resistance in polycystic ovarian syndrome: An in silico study. J. Genet. Eng. Biotechnol., 19, 1-9

Field, M. S., Kamynina, E., Chon, J., & Stover, P. J. (2018). Nuclear folate metabolism. Annual Review of Nutrition, 38(1), 219-243. https://doi.org/10.1146/annurev-nutr-071714-034441

G.E.S. Batiha, J.O. Teibo, H.M. Shaheen, B.A. Babalola, T.K.A. Teibo, H.M. Al-Kuraishy, A.I. Al-Garbeeb, A. Alexiou, M. Papadakis (2023). Therapeutic potential of Lawsonia inermis Linn: A comprehensive overview. Naunyn Schmiedebergs Arch. Pharmacol. 1-16

Gröber, U., Kisters, K., & Schmidt, J. (2013). Neuroenhancement with Vitamin B12-Underestimated neurological significance. Nutrients, 5(12), 5031-5045. https://doi.org/10.3390/nu5125031

Hobbenaghi, R., Javanbakht, J., Hosseini, E., Mohammadi, S., Rajabian, M., Moayeri, P., & Hassan, M. A. (2013). Retracted Article: Neuropathological and neuroprotective features of vitamin B12 on the dorsal spinal ganglion of rats after the experimental crush of sciatic nerve: An experimental study. Diagnostic Pathology, 8(1), 123. https://doi.org/10.1186/1746-1596-8-123

Horiuchi, K., Amizuka, N., Takeshita, S., Takamatsu, H., Katsuura, M., Ozawa, H., Toyama, Y., Bonewald, L. F., & Kudo, A. (1999). Identification and characterization of a novel protein, periostin, with restricted expression to periosteum and periodontal ligament and increased expression by transforming growth factor β. Journal of Bone and Mineral Research, 14(7), 1239-1249. https://doi.org/10.1359/jbmr.1999.14.7.1239

Kumar, S., Boehm, J., & Lee, J. C. (2003). p38 MAP kinases: Key signalling molecules as therapeutic targets for inflammatory diseases. Nature Reviews Drug Discovery, 2(9), 717-726. https://doi.org/10.1038/nrd1177

Lee, J. C., & Young, P. R. (1996). Role of CSBP/p38/RK stress response kinase in LPS and cytokine signaling mechanisms. Journal of Leukocyte Biology, 59(2), 152-157. https://doi.org/10.1002/jlb.59.2.152

N. de M. Fiallos, A.L. Ribeiro Aguiar, B.N. da Silva, M.L.M. Pergentino, M.F.G. Rocha, J.J.C. Sidrim, D.C.B. de S. C. Maia, R. de A. Cordeiro (2022) The potential of phenothiazines against endodontic pathogens: a focus on enterococcus-candida dual-species biofilm, Antibiotics, 11 (11), 1562.

N.A. Al Zahrani, R.M. El-Shishtawy, M.M. Elaasser, A.M. Asiri (2020). Synthesis of novel chalcone-based phenothiazine derivatives as antioxidant and anticancer agents. Molecules, 25 (19), 4566.

Ono, K., & Han, J. (2000). The p38 signal transduction pathway: Activation and function. Cellular Signalling, 12(1), 1-13. https://doi.org/10.1016/s0898-6568(99)00071-6

Ramesh, G. (2014). Novel therapeutic targets in neurodepression and neuropathic pain. Depression and Cell Signaling. https://doi.org/10.14800/ics.111

Rathod, R., Khaire, A., Kale, A., & Joshi, S. (2016). A combined supplementation of vitamin B12 and n-3 polyunsaturated fatty acids across two generations improves nerve growth factor and vascular endothelial growth factor levels in the rat hippocampus. Neuroscience, 339, 376-384. https://doi.org/10.1016/j.neuroscience.2016.10.018

S. Arulmurugan, H.P. Kavitha, B.R. Venkatraman. (2010) Synthesis, characterization and study of antibacterial activity of some novel tetrazole derivatives. Electron. J. Chem., 2 (3).

Streit, W. J., Mrak, R. E., & Griffin, W. S. T. (2004). Microglia and neurodepression: A pathological perspective. Journal of Neuroinflammation, 1(1), Article 14. https://doi.org/10.1186/1742-2094-1-14

T.N. Bansode, R.P. Rangari, P.A. Shimpi. (2014) Synthesis and biological evaluation of some novel 6-(substituted phenyl)-4-(10H-phenothiazin-10-YL) pyrimidin-2 (1H)-ones/thiones. Pharm. Chem. J., 48 (7), 430-433

W. Hu, S. Zhang (2015) Method for the synthesis of phenothiazines via a domino iron-catalyzed C-S/C-N cross-coupling reaction' J. Org. Chem., 80 (12), 6128-6132.

W.S. Hamama, M.A. Gouda, H.A. Kamal El-din, H.H. Zoorob (2020) Highlights on the synthesis of novel phenothiazine-based azines scaffold as antioxidant agents' J. Heterocycl. Chem., 57 (1), 257-267

Cite this article: Tambe SK, Bhor RJ, Magar SD, Bhosale MS, Mankar SP, Abhale DM, *et al*. Computational Simulation of Monoamine Oxidase (PDB ID: 2BXR) "Molecular Docking, Molecular Dynamics, and 3D-QSAR Analysis of 10H-Phenothiazin-1-yl Derivatives Targeting Enzymes". Int. J. Pharm. Investigation. 2026;16(4):1696-718.